

Two-probe theory of scanning tunneling microscopy of single molecules: Zn(II)-etioporphyrin on alumina

John Buker and George Kirczenow

Department of Physics, Simon Fraser University, Burnaby, British Columbia, Canada, V5A 1S6

(September 12, 2018)

Abstract

We explore theoretically the scanning tunneling microscopy of single molecules on substrates using a framework of two *local* probes. This framework is appropriate for studying electron flow in tip/molecule/substrate systems where a thin insulating layer between the molecule and a conducting substrate transmits electrons non-uniformly and thus confines electron transmission between the molecule and substrate laterally to a nanoscale region significantly smaller in size than the molecule. The tip-molecule coupling and molecule-substrate coupling are treated on the same footing, as local probes to the molecule, with electron flow modelled using the Lippmann-Schwinger Green function scattering technique. STM images are simulated for various positions of the stationary (substrate) probe below a Zn(II)-etioporphyrin I molecule. We find that these images have a strong dependence on the substrate probe position, indicating that electron flow can depend strongly on both tip position and the location of the dominant molecule-substrate coupling. Differences in the STM images are explained in terms of the molecular orbitals that mediate electron flow in each case. Recent experimental results, showing STM topographs of Zn(II)-etioporphyrin I on alumina/NiAl(110) to be strongly dependent on which individual molecule on the substrate is being probed, are explained using this model. A further experimental test of the model is also proposed.

PACS: 68.37.Ef, 85.65.+h, 73.63.Rt, 68.43.Fg

Typeset using REVTeX

I. INTRODUCTION

In the last 20 years, scanning tunneling microscopy has become an increasingly valuable tool for studying electron transport through individual molecules. Experiments in this area of research involve the adsorption of molecules onto a substrate and analysis using an STM tip to probe the system. Some early examples are found in Refs. 1–5. The last 5-10 years has seen the emergence of a true wealth of such experiments on many different molecular systems^{6,7}. In a simplified picture of transport through an STM tip/molecule/substrate system, when a finite potential bias is applied between the tip and the substrate, the tip and substrate electrochemical potentials separate and molecular orbitals located in the window of energy between the two electrochemical potentials mediate electron flow between the tip and the substrate. In this way, experimental data such as current-voltage characteristics may give clues to the electronic structure of the molecule.

A more complete understanding of these tip/molecule/substrate systems is complicated by the fact that the molecule may interact strongly with the tip and substrate, and in that case one should not think of the molecule as being an isolated part of the system. Electron flow has been shown to be dependent on the details of the tip and substrate molecular coupling^{8–14}. In experiments on planar or near-planar molecules, constant current or constant height topographic STM images of sub-molecular resolution^{2,12,13,15–19} show how current flow through a molecule is dependent on the lateral position of the STM tip above the molecule. These topographic images may also depend on details of the molecule/substrate configuration. For example, STM experiments on “lander” molecules on a Cu(111) surface¹⁴ show differences in topographic images when a molecule is moved towards a step edge.

Theoretical approaches to modeling STM-based electron flow commonly treat the tip as a probe of the molecule-substrate system. The Bardeen²⁰ approximation considers the tip and sample to be two distinct systems that are perturbed by an interaction Hamiltonian. Techniques such as the Tersoff-Hamann formalism²¹ calculate a tunneling current based on the local density of states (LDOS) of the tip and of the sample. Such approaches are widely used and have been very productive for the understanding of these systems. There has correspondingly been much interest in studying the tip-molecule interaction and the details of the coupling. Theoretical and experimental results in this area can be readily compared by comparing real and simulated STM topograph maps. Details of the molecule-substrate coupling may also affect the the image of the molecule. A number of different theoretical approaches^{22–27} have been developed that predict effects of molecule-substrate coupling^{8–11,14}, in experimental situations where the geometry of the substrate is homogeneous. In many of these experimental situations, a molecule is placed on a metal substrate, resulting in strong coupling along the entire molecule-metal interface. More recently, experimental systems of molecules placed on thin insulating layers above the metal part of the substrate have allowed the mapping of HOMO-LUMO orbitals of the molecule as well as the study of molecular electroluminescence^{16–19,28}. Some of these systems involve relatively simple substrates, including an insulating layer that behaves qualitatively like a uniform tunnel barrier^{18,19} and considerable progress has been made understanding their STM images. Others, with planar molecules on alumina/metal substrates, have more complex images^{16,17} that depend on the precise location of the molecule on the substrate and are much less well-understood. STM images of thin (5Å) *pristine* alumina films on NiAl(111) surfaces exhibit

regular arrays of bright spots²⁹ that signal locations where the film is the most conductive. The most conductive locations are spaced 15 to 45Å apart depending on the bias voltage applied between the STM tip and substrate.²⁹ Thin alumina films on NiAl(110) surfaces have similar small, relatively conductive regions, although in this case they do not form simple periodic patterns, presumably because the structure of the alumina film is not commensurate with the NiAl(110) substrate.³⁰ Thus it is reasonable to suppose that for such systems the alumina film behaves as an *non-uniform* tunnel barrier between a molecule on its surface and a metal substrate beneath it and that electrons are transmitted between the molecule and substrate primarily at the more conductive spots of the alumina film. If the adsorbed planar molecule is similar in size to the average spacing between the most conductive spots of the alumina film (this is the case for the Zn(II)-etioporphyrin I molecules studied experimentally in Ref. 16), then a *single* conductive spot of the film can dominate the electronic coupling between a suitably placed molecule and the underlying metal substrate. Thus, as is shown schematically in Fig. 1, in an STM experiment on such a system not only the STM tip but also the substrate should be regarded as a *highly local* probe making direct electrical contact with a small part of the molecule. Therefore conventional STM experiments on such systems can in principle yield information similar to that from experiments probing a single molecule simultaneously with *two* separate atomic STM tips, which are beyond the reach of present day technology. In this article, we propose a simple approach for modeling such systems that should be broadly applicable, and use it to explain the results of recent experiments.¹⁶

We re-examine scanning tunneling microscopy of molecules, treating the tip-molecule coupling and the molecule-substrate coupling on the same footing, both as *local* probes of the molecule, as is shown schematically in Fig. 2. In this two-probe model, the probes are represented using a one-dimensional tight-binding model, and electron flow is modelled using the Lippmann-Schwinger Green function scattering technique. We find that the STM image of a molecule can be sensitive to the location of the dominant molecule-substrate coupling.

We present results for the Zn(II)-etioporphyrin I molecule, treated with extended Hückel theory. STM-like images are created by simulating movement of the tip probe laterally above the molecule while keeping the substrate probe at a fixed position below the molecule. We obtain different current maps for various positions of the stationary (substrate) probe, and explain their differences in terms of the molecular orbitals that mediate electron flow in each case. Our results are shown to be consistent with recent experimental STM imagery for the system of Zn(II)-etioporphyrin I on an alumina-covered NiAl(110) substrate¹⁶. By using the two-probe approach described in this article, we are able to account for all of the differing types of topographic maps that are seen when this molecule is adsorbed at different locations on the substrate. However, despite the success of our model in accounting for the observed behavior of this system, we emphasize that a detailed microscopic knowledge of exactly how the Zn(II)-etioporphyrin I molecules interact with the alumina-covered NiAl surface is still lacking and we hope that the present study will stimulate further experimental/theoretical elucidation of this system. We propose an experiment that may shed additional light on this issue at the end of this article.

II. THE MODEL

In the present model, the tip and substrate are represented by probes, with each probe modelled as a one-dimensional tight-binding chain, as is depicted in Fig. 3. The molecule is positioned between the probes, so that it mediates electron flow between the tip and substrate. The model Hamiltonian of this system can be divided into three parts, $H = H_{probes} + H_{molecule} + W$, where W is the interaction Hamiltonian between the probes and the molecule. The Hamiltonian for the probes is given by

$$H_{probes} = \sum_{n=-\infty}^{-1} \epsilon_{tip} |n\rangle\langle n| + \beta(|n\rangle\langle n-1| + |n-1\rangle\langle n|) + \sum_{n=1}^{\infty} \epsilon_{substrate} |n\rangle\langle n| + \beta(|n\rangle\langle n+1| + |n+1\rangle\langle n|), \quad (1)$$

where ϵ_{tip} and $\epsilon_{substrate}$ are the site energies of the tip and substrate probes, β is the hopping amplitude between nearest neighbour probe atoms, and $|n\rangle$ represents the orbital at site n of one of the probes. We take the electrochemical potentials of the tip and substrate probes to be $\mu_T = E_F + eV_{bias}/2$ and $\mu_S = E_F - eV_{bias}/2$, where V_{bias} is the bias voltage applied between them and E_F is their common Fermi level at zero applied bias. The applied bias also affects the site energies ϵ_{tip} and $\epsilon_{substrate}$ so that $\epsilon_{tip} = \epsilon_{0,tip} + eV_{bias}/2$ and $\epsilon_{substrate} = \epsilon_{0,substrate} - eV_{bias}/2$, where $\epsilon_{0,tip}$ and $\epsilon_{0,substrate}$ are the site energies of the tip and substrate probes at zero bias. In this model, the potential drop from the tip probe to the molecule, and from the molecule to the substrate, are assumed to be equal, and there is no potential drop within the molecule.³¹ Thus, the molecular orbital energies are considered to be fixed when a bias voltage is applied. The Hamiltonian of the molecule may be expressed as

$$H_{molecule} = \sum_j \epsilon_j |\phi_j\rangle\langle\phi_j|, \quad (2)$$

where ϵ_j is the energy of the j^{th} molecular orbital ($|\phi_j\rangle$). The interaction Hamiltonian between the probes and molecule is given by

$$W = \sum_j W_{-1,j} |-1\rangle\langle\phi_j| + W_{j,-1} |\phi_j\rangle\langle-1| + W_{j,1} |\phi_j\rangle\langle 1| + W_{1,j} |1\rangle\langle\phi_j|, \quad (3)$$

where $W_{-1,j}$, $W_{j,-1}$, $W_{j,1}$ and $W_{1,j}$ are the hopping amplitude matrix elements between the probes and the various molecular orbitals $|\phi_j\rangle$.

Electrons initially propagate through one of the probes (which we will assume to be the tip probe) toward the molecule in the form of Bloch waves, and may either undergo reflection or transmission when they encounter the molecule. Their wavefunctions are of the form

$$|\psi\rangle = \sum_{n=-\infty}^{-1} (e^{iknd} + r e^{-iknd}) |n\rangle + \sum_{n=1}^{\infty} t e^{ik'nd} |n\rangle + \sum_j c_j |\phi_j\rangle \quad (4)$$

where d is the lattice spacing, and t and r are the transmission and reflection coefficients. Upon transmission, the wavevector k changes to k' due to the difference in site energies ϵ_{Tip}

and $\epsilon_{Substrate}$ of the tip and substrate probes. The transmission probability is given by

$$T = |t|^2 \left| \frac{v(k'd)}{v(kd)} \right| = |t|^2 \frac{\sin(k'd)}{\sin(kd)} \quad (5)$$

where $v(k)$ and $v(k')$ are the respective velocities of the incoming and transmitted waves.

The transmission amplitude t may be evaluated by solving a Lippmann-Schwinger equation for this system,

$$|\psi\rangle = |\phi_0\rangle + G_0(E)W|\psi\rangle, \quad (6)$$

where $G_0(E) = (E - (H_{probes} + H_{molecule}) + i\delta)^{-1}$ is the Green function for the decoupled system (without W), and $|\phi_0\rangle$ is the eigenstate of an electron in the decoupled tip probe. $G_0(E)$ may be separated into the three decoupled components: the tip and substrate probes, and the molecule. For the tip/substrate probes,

$$G_0^{Tip/Substrate} = \sum_k \frac{|\phi_0(k)\rangle\langle\phi_0(k)|}{E - (\epsilon_{Tip/Substrate} + 2\beta\cos(kd))} \quad (7)$$

where d is the lattice spacing and $\epsilon_{Tip/Substrate} + 2\beta\cos(kd)$ is the energy of a tip/substrate electron with wavevector k . For the molecule,

$$G_0^M = \sum_j \frac{|\phi_j\rangle\langle\phi_j|}{E - \epsilon_j} = \sum_j (G_0^M)_j |\phi_j\rangle\langle\phi_j|. \quad (8)$$

The transmission probability for such a system using this formalism has been previously solved³³, and found to be equal to

$$T(E) = \left| \frac{A(\phi_0)_{-1}}{[(1-B)(1-C) - AD]} \right|^2 \frac{\sin(k'_0 d)}{\sin(k_0 d)} \quad (9)$$

where $(\phi_0)_{-1} = \langle -1|\phi_0\rangle$, and

$$\begin{aligned} A &= (e^{ik'_0 d}/\beta) \sum_j W_{1,j} (G_0^M)_j W_{j,-1} \\ B &= (e^{ik'_0 d}/\beta) \sum_j (W_{1,j})^2 (G_0^M)_j \\ C &= (e^{ik_0 d}/\beta) \sum_j (W_{-1,j})^2 (G_0^M)_j \\ D &= (e^{ik_0 d}/\beta) \sum_j W_{-1,j} (G_0^M)_j W_{j,1}. \end{aligned} \quad (10)$$

Here, k_0 is the wavevector of an electron in the tip probe with energy E , and k'_0 is the wavevector of an electron in the substrate probe, of the same energy E .

In the present work, molecular orbitals are evaluated using extended Hückel theory³² and therefore require a non-orthogonal basis set within the molecule. It has been shown that a simple change of Hilbert space can redefine the problem in terms of a system with an

orthogonal basis³³. This is achieved by transforming the Hamiltonian of the system into a new energy-dependent Hamiltonian H^E :

$$H^E = H - E(S - I) \quad (11)$$

where H is the original Hamiltonian matrix, S is the overlap matrix, and I is identity. In the model presented here, we assume orthogonality between the orbitals of the probe leads, although by using Eq.(11) the model could easily be extended to systems where these orbitals of the probe are non-orthogonal.

By using the Lippmann-Schwinger approach, we are free to choose convenient boundaries for the central scattering region, not necessarily restricted to the actual molecule. In order to model the coupling between the probes and molecule in a realistic way, we consider the probe atoms that are closest to the molecule to be part of an *extended molecule* (see Fig. 3), i.e., we treat them as if they were parts of the molecule. Their orbitals $|a\rangle$ and $|b\rangle$ are assumed to be orthogonal to the lead orbitals $|-1\rangle$ and $|1\rangle$ on the lead sites adjacent to them.

Then, we have

$$\begin{aligned} W_{-1,j} = W_{j,-1} &= \langle -1|H|a\rangle\langle a|\phi_j\rangle = \beta c_{a,j} \\ W_{j,1} = W_{1,j} &= \langle \phi_j|b\rangle\langle b|H|1\rangle = \beta c_{b,j}. \end{aligned} \quad (12)$$

In order to calculate the electric current passing through an STM/molecule/substrate system, the transmission probability of an electron, $T(E)$, is integrated through the energy range inside the Fermi energy window between the two probes that is created when a bias voltage is applied. To obtain a theoretical STM current map, this electric current calculation is performed for many different positions of the tip probe, while the substrate probe remains stationary. The simplicity of this model allows a complete current map to be generated in a reasonable amount of time. By comparing current maps that are generated for different substrate probe configurations, we are able to develop an intuitive understanding of the important role substrates may play in STM experiments on single molecules.

In the remainder of this paper, we will consider, as an example, a molecule of current experimental interest¹⁶, Zn(II)-etioporphyrin I. For simplicity, we model the probes as consisting of Cu s-orbitals, and compare various simulated constant-height STM current maps of the molecule obtained using different substrate probe locations, corresponding to different possible locations of dominant molecule-substrate coupling. We will demonstrate how the properties of an STM current image may display a remarkable qualitative dependence on the location of this molecule-substrate coupling.

III. MODEL RESULTS

We present results for the single-molecule system of Zn(II)-etioporphyrin I (ZnEtioI) (see Fig. 4), coupled to model tip and substrate probes that we represent for simplicity by Cu s-orbitals. Density functional theory was used in obtaining the geometrical structure of ZnEtioI³⁴. The molecule is mainly planar, but contains 4 out-of-plane ethyl groups.

The electronic structure of the molecule was computed using the extended Hückel model³². In this model, the energy of the highest occupied molecular orbital (HOMO) was found to be -11.5 eV, and the energy of the lowest unoccupied molecular orbital (LUMO) was found to be -10.0 eV. The Fermi level of a metallic probe in contact with a molecule at zero applied bias is usually located between molecular HOMO and LUMO levels. However, establishing the precise position of the Fermi energy of the probes relative to the HOMO and LUMO is in general a difficult problem in molecular electronics, with different theoretical approaches yielding differing results^{35–37}. Therefore, within this illustrative model, we consider two possible zero-bias Fermi energy positions for the probes: In the *LUMO-energy transmission* subsection (III A), the Fermi energy is taken to be -10.4 eV³⁸. Thus, at $V_{bias} = 1.0$ V, the Fermi energy window will include the LUMO but not the HOMO. In the *HOMO-energy transmission* subsection (III B), the Fermi energy is taken to be -11.4 eV. In this case, at $V_{bias} = 1.0$ V, the Fermi energy window will include the HOMO but not the LUMO.³⁹

A. LUMO-energy transmission

We first consider the case of transmission through the molecule at LUMO energies. For this, we set $V_{bias} = 1.0$ V, with $E_F = -10.4$ eV at zero bias. The substrate probe is now positioned to simulate various possible locations of dominant molecule-substrate coupling. Four different positions for the substrate probe are analyzed, as shown by the blue circles in Fig. 4: directly below one of the outer ethyl groups of the molecule (A), below an inner carbon atom of the molecule (B), below a nitrogen atom (C), and below the zinc center of the molecule (D). The orbital representing the substrate probe, in each case, is centered 2.5Å below the nearest atom in the molecule. Constant-height STM current images for these substrate probe positions are simulated by moving the tip probe across the molecule in steps of 0.25Å, calculating the electric current at each step, thus creating a 16Å×16Å electric current image (transmission pattern). The tip probe in all cases is located 2.5Å above the plane of the molecule.

Fig. 5(a,b,c,d) shows the simulated current images obtained in each case, the blue circle indicating the position of the substrate probe. Each image has unique features not seen in the other images, that arise due to differences in the details of the molecule-substrate coupling. In Fig. 5(a), with the substrate probe positioned below an outer ethyl group as shown in Fig. 4 (position A), a delocalized transmission pattern is obtained. A localized region of enhanced transmission exists where the tip probe is directly above the same ethyl group that is coupled to the substrate probe. In Fig. 5(b), a somewhat similar transmission lobe pattern is obtained, with the substrate probe positioned below an inner carbon atom (see Fig. 4, position B). In this configuration, however, the transmission pattern has two-fold

symmetry and there is no apparent localized region of enhanced transmission. Furthermore, the lobes of high transmission in Fig. 5(b) are 1-2 orders of magnitude stronger than the corresponding lobes in Fig. 5(a), as will be discussed below. In the case when the substrate probe is directly below a nitrogen atom (see Fig. 4, position C), a distinct transmission pattern is obtained, shown in Fig. 5(c). The lobe with the highest transmission in this figure is 1-2 orders of magnitude weaker than lobes seen in Fig. 5(b). In this case, a localized region of enhanced transmission exists where the tip probe is above the same nitrogen atom that is coupled to the substrate probe. Fig. 5(d) shows a very different transmission pattern. In this case, the substrate probe is positioned directly below the center zinc atom of the molecule (Fig. 4, position D), and transmission is found to occur primarily when the tip probe is above the center of the molecule.

In order to help understand the differences between these images, the characteristics of the LUMO were investigated. The LUMO is a degenerate π -like orbital with two-fold symmetry. Analyzing the LUMO as a linear combination of atomic orbitals, we find that contributions to the LUMO come primarily from atomic orbitals in the core porphyrin structure, with low contributions from the ethyl groups and the central zinc atom. Particularly high contributions come from two of the four inner corner carbon atoms (the atom above substrate probe B and the corresponding atom 180 degrees away, in Fig. 4, or the equivalent atoms under rotation of 90 degrees for the other degenerate LUMO orbital). Therefore, in the case of Fig. 5(b), there is a strong coupling between the substrate probe and one of the two degenerate LUMOs of the molecule, whereas in the case of Fig. 5(a), with the substrate probe below the ethyl group, there is only a weak substrate-LUMO coupling. This explains why the transmission pattern of Fig. 5(b) is much stronger than Fig. 5(a). Regarding the similar appearance of the transmission patterns in the two cases, we expect LUMO-mediated transmission to occur, in both cases, when the tip probe has significant coupling to the LUMO. The delocalized transmission patterns of Fig. 5(a) and Fig. 5(b) in fact correspond well to areas of high atomic orbital contributions to the LUMO, with the low-transmission nodes occurring in regions of the molecule where the amplitude of the LUMO is close to zero.

The differences between the transmission patterns may be better understood by studying $T(E)$ for appropriate tip probe positions in each case. Fig. 5(e,f,g,h) shows $T(E)$ for the corresponding placement of the tip probe as labelled by red dots in Fig. 5(a,b,c,d). In Fig. 5(e), $T(E)$ is shown for the localized region of enhanced transmission in Fig. 5(a). There is a transmission resonance associated with the LUMO (at -10 eV), together with an antiresonance that occurs at a slightly lower energy. The antiresonance, along with antiresonances seen in subsequent figures (with the exception of the antiresonance in Fig. 5(f)), arises due to interference between electron propagation through a weakly coupled orbital (in this case the LUMO) and propagation through other orbitals of different energies. This can be seen mathematically through Eq.(9) and Eq.(10). Transmission drops to 0 when $A = 0$. This occurs when all the terms $W_{1,j}(\frac{1}{E-\epsilon_j})W_{j,-1}$ for the different orbitals sum to 0. If an orbital is weakly coupled to the probes, its contribution to A is small unless the electron energy is close to the energy of the orbital. When the electron energy does approach this orbital energy, the contribution to A will increase and, if its sign is opposite, cancel the other orbitals' contributions. Thus, these types of antiresonances are always seen on only one side

of a transmission peak of a weakly coupled orbital. Returning to Fig. 5(e), we see that, although transmission via the LUMO contributes some of the electric current, a significant contribution comes from the background. We find this background transmission to be composed primarily of the high energy transmission tails of molecular orbitals localized on the ethyl groups. When the tip probe is coupled to the same ethyl group as the substrate probe, transmission via these ethyl-composed molecular orbitals is strong and has a significant tail extending to the relevant range of energies near the LUMO. Fig. 5(f) shows $T(E)$ for the same tip probe position as Fig. 5(e), but with the substrate probe positioned below an inner carbon atom, as in Fig. 5(b). Since the substrate probe is not significantly coupled to the ethyl group, the ethyl-based transmission background is negligible, and the region of locally enhanced transmission seen in Fig. 5(a) is not seen in Fig. 5(b). It should also be noted that the transmission peak in Fig. 5(f) is wider than in Fig. 5(e), due to hybridization of the LUMO with the strongly coupled substrate probe. The antiresonance seen at the center of the peak is due to the degeneracy of the LUMO. In this case, one of the LUMO orbitals is strongly coupled to the substrate probe, with the other being only weakly coupled. The weakly coupled orbital causes electron backscattering to occur, resulting in an antiresonance at the LUMO energy. In Fig. 5(g), the substrate probe is directly below a nitrogen atom and the tip probe directly above. In this case, the transmission peak corresponding to the LUMO is very narrow, and current flow comes primarily from background transmission. This background transmission corresponds mainly to the high energy transmission tails of molecular orbitals that have strong contributions from the nitrogen atoms. The transmission pattern seen in Fig. 5(c) is the result of contributions from these various low-energy orbitals, and from the HOMO-1 and HOMO-2, which will be analyzed in greater detail in subsection III B. Transmission through the LUMO is quenched because the substrate probe is coupled to a region of the molecule where the amplitude of the LUMO is close to zero. Thus, the overall transmission pattern is weak compared to Fig. 5(b). In Fig. 5(h), the substrate probe is directly below the center of the molecule and the tip probe directly above. For this case, the transmission curve contains no LUMO-related transmission peak, since the LUMO is an antisymmetric orbital and has a node at the center of the molecule. Instead, we see a transmission background that rises smoothly with energy. This transmission corresponds to the tail of a higher-energy π -like orbital composed primarily of zinc, with additional, less-significant contributions from other atoms. The transmission pattern of Fig. 5(d), plotted on a log scale, is shown in Fig. 6, and reveals additional structure of this orbital. Transmission through this orbital has delocalized features not evident in Fig. 5(d), such as nodes of low transmission when the tip probe is above a nitrogen atom, as well as regions of higher transmission when the tip probe is above the outer sections of the molecule. In Fig. 5(h), the probes are both coupled strongly to this orbital, so the orbital hybridizes with the probes and creates a transmission peak with a very long tail. Compared to this tail, transmission via the LUMO (which has very low zinc content) is negligible.

B. HOMO-energy transmission

Next, we consider electron transmission at energies close to the HOMO. For the purposes of analyzing HOMO-mediated transmission, we consider the probes to have a zero-bias Fermi

energy of -11.4 eV, which is closer to the HOMO than the LUMO. We again set $V_{bias} = 1.0$ V, and consider the same four cases of substrate probe position as for transmission at LUMO energies.

The HOMO of zinc-etiochlorin is a non-degenerate π -like orbital with 4-fold symmetry and an energy of -11.5 eV. The primary atomic contributions to this orbital are from carbon atoms in the 4 pyrrole rings, with weak contributions from the ethyl groups and negligible contributions from all of the other inner atoms. In the energy window we are considering, there exists another π -like orbital (HOMO-1), also 4-fold symmetric and with an energy of -11.8 eV. Unlike the HOMO, this orbital has large contributions from the inner corner carbon atoms (see Fig. 4, above position B, and symmetric equivalents). It also has significant contributions from the nitrogen atoms, as well as non-negligible contributions from the zinc center and the 4 ethyl groups. In this energy range, there is also a σ -like orbital (HOMO-2) at an energy of -11.9 eV, with strong contributions from the nitrogen atoms.

Transmission patterns for this energy range are shown in Fig. 7(a,b,c,d), corresponding to the same substrate probe positions as in Fig. 5(a,b,c,d). In the case where the substrate probe is directly below an ethyl group (Fig. 7(a)), a complex transmission pattern is obtained. In particular, low-transmission nodes exist every 45 degrees. To understand the source of these nodes, $T(E)$ is shown (see Fig. 7(e)) for two different tip probe positions that are very close to each other, one being directly on a node (the red dot in Fig. 7(a)) and the other a small distance away but in a region of higher transmission (the black dot). Note that $T(E)$ is shown, in this case only, in the narrower energy range of -11.9 eV to -11.4 eV. (No transmission peaks are present in the energy range from -11.4 eV to -10.9 eV.) We see that transmission through the HOMO is extremely quenched (the transmission peak narrows) when the tip probe is above the node, but transmission through the HOMO-1 is relatively unaffected. (The very narrow -11.88 eV transmission peak corresponding to the σ -like HOMO-2 orbital has a negligible effect on overall current flow.) This quenching of transmission through the HOMO occurs because the tip probe is closest to a region of the molecule where the HOMO's amplitude is nearly zero. These regions occur every 45 degrees, as shown by the nodes. The other (curved) low-transmission nodes that are seen in Fig. 7(a) are caused by the HOMO-1, as will become clear through analysis of Fig. 7(b). Since both the HOMO and HOMO-1 are coupled non-negligibly to the substrate probe in Fig. 7(a), we see a transmission pattern that is affected by both of these orbitals. In the case (Fig. 7(b)) when the substrate probe is below an inner corner carbon atom (Fig. 4, position B), a transmission pattern that is significantly different from Fig. 7(a) is obtained. The low-transmission nodes every 45 degrees are not seen, and there are strong transmission peaks when the tip probe is above one of the 4 inner corner carbon atoms. In Fig. 7(f), $T(E)$ is shown for the case when the tip probe and substrate probe are directly above and below the same corner carbon atom. The HOMO-1 is clearly the dominant pathway for transmission through the molecule, with the HOMO and HOMO-2 producing only narrow additional transmission peaks. This is understandable, since the corner carbon atom which is closest to both the tip and substrate probes has a negligible contribution to the HOMO, but a large contribution to the HOMO-1. Hence, the transmission pattern seen in Fig. 7(b) is primarily due to (HOMO-1)-mediated transmission through the molecule. The curved low transmission nodes correspond to regions of the molecule where the amplitude of the HOMO-1 is close to 0. Similar curved low-transmission nodes are also seen in Fig. 7(a),

illustrating that the HOMO-1 is also the source of these nodes. In the case when the substrate probe is below a nitrogen atom, another unique transmission pattern is obtained. In Fig. 7(g), $T(E)$ is shown for the case when the tip probe and substrate probe are above and below the same nitrogen atom. Two transmission peaks of similar strength are seen, corresponding to the HOMO-1 and HOMO-2, as well as a very weak peak corresponding to the HOMO. This is understandable, since both the HOMO-1 and HOMO-2 have considerable nitrogen contributions, and the HOMO does not. Hence, the transmission pattern seen in Fig. 7(c) is due to both the HOMO-1 and HOMO-2, resulting in a unique transmission pattern. Lastly, when the substrate probe is below the center of the molecule (Fig. 7(d)), a transmission pattern looking quite similar to Fig. 7(b) is obtained. Unlike in the case of LUMO energies, the transmission pattern for HOMO energies is not dominated by transmission through the low-energy tail of a zinc-dominated orbital. Rather, transmission appears to be mediated mainly by the HOMO-1 orbital. This is because the HOMO-1, unlike the HOMO or LUMO, has non-negligible contributions from the center zinc atom, that is strongly coupled to the substrate probe in this case. In Fig. 7(h), $T(E)$ is shown for the case of the tip probe and substrate probe being directly above and below the center of the molecule. We see a main transmission peak corresponding to the HOMO-1, as well as a background due to the tail of the higher-energy zinc-dominated orbital. This results in stronger transmission when the tip is above the center of the molecule than if only the HOMO-1 is strongly coupled to the substrate probe, as occurs in Fig. 7(b).

All of the unique features seen in each of these four cases, for both HOMO and LUMO energy ranges, directly arise from differences in the details of the molecule-substrate coupling in each case. While an individual substrate probe positioned below the molecule is an incomplete representation for the molecule-substrate interaction, this representation illustrates the importance of understanding the detailed nature of the molecule-substrate interaction when analyzing and modeling STM topographs of single molecules on substrates. Nevertheless, specific experimental results can indeed be shown to be consistent with results of the model presented in this article, as will be discussed next.

C. Comparison with Experiment

STM transmission patterns for the system of Zn(II)-etioporphyrin I adsorbed on inhomogeneous alumina covering a NiAl(110) substrate have recently been obtained experimentally¹⁶. These experimental results generally show four lobes above the etioporphyrin molecule, where placement of the STM tip results in high transmission. Experimentally, the relative transmission through each of the lobes is found to depend strongly on which individual molecule is being probed, due to the complex nature of the alumina-NiAl(110) substrate. Often, one or two lobes are found to have much higher transmission than the rest. These asymmetries were originally attributed to conformational differences between molecules. However, a further investigation of conformational differences only identified different molecular conformations that produce *two-fold symmetric* patterns⁴⁰. Thus, a different explanation is needed for the images of lower symmetry seen on the alumina.

An alternate explanation for the various different STM images obtained for individual molecules will now be presented. In the experiments, the molecules were likely more strongly

coupled to the substrate than to the STM tip, since the molecules were adsorbed on the substrate, and the experiments were performed at a relatively low tunneling current of 0.1 nA. The STM images were obtained at positive substrate bias, therefore we may infer that the lobes represent regions of strong transmission around *LUMO energies*. The experimental results are consistent with the two-probe model results for the situation shown in Fig. 5(a) (at LUMO energies, with the substrate probe placed below one of the out-of-plane ethyl groups of the molecule), as will be explained below. To more realistically model what one might see in an STM experiment with finite lateral resolution, the resolution of Fig. 5(a) should be reduced: Fig. 8 shows the same transmission pattern as Fig. 5(a), but in convolution with a gaussian weighting function of width 6Å. We see that two distinct high transmission lobes emerge, one much stronger than the other, about 11Å apart. Experimentally, the most common image seen by Qiu et al. (Fig. 2B in their article¹⁶) is, after an appropriate rotation, remarkably similar to Fig. 8, also containing two dominant asymmetric lobes, located 11Å apart.

The other less-common STM images observed experimentally can also be explained qualitatively with our model. In an experimental situation, the underlying metal substrate may be coupled to *all four* ethyl groups at significantly differing strengths depending on the detailed local arrangement and strengths of the most conductive spots of the alumina film (discussed in Section I) in the vicinity of the molecule. The result would resemble a superposition of Fig. 8 and current maps derived from Fig. 8 by rotation through 90, 180, and 270 degrees, with weights depending on the relative strength of the coupling of the substrate to each of the ethyl groups.⁴¹ In this analysis, other substrate probe positions that are the same distance from the plane of the molecule (about 4Å) but not below an ethyl group have also been considered. It was found that other substrate probe positions yielded much weaker current flow through the molecule. Thus, these positions can be neglected in a first approximation, and current flow can be assumed to be dominated by pathways through the four substrate probe positions below the ethyl groups. All of the different transmission pattern results obtained experimentally can be reproduced in this way reasonably well, given the simplicity of the model and the fact that the model results are for constant-height calculations whereas experimentally, constant-current STM images are obtained.

One final consideration is that in an experimental situation, the out-of-plane ethyl groups of the Zn-etiochlorophyll molecule may possibly point *away* from the substrate, contrary to what has been assumed above. Thus, we now consider this case. Fig. 9 shows transmission patterns that correspond to the four substrate probe positions shown in Fig. 4, assuming the ethyl groups point *away* from the substrate probe. The substrate probe is positioned 2.5Å below the plane of the molecule, and the tip probe scans the molecule at a constant height of 4Å above the plane. We see that in the case of Fig. 9(a), two asymmetric lobes corresponding to the out-of-plane ethyl groups dominate the image, one about double the strength of the other. In Fig. 9(b,c), two symmetric ethyl-based lobes dominate the images, with strengths similar to the strength of the weaker lobe of Fig. 9(a). In Fig. 9(d), however, current flows primarily through the center of the molecule, again with a strength similar to that of the weaker lobe of 9(a). Thus, we see that most substrate probe positions (other than below the center of the molecule) produce current patterns with high-transmission lobes corresponding to the locations of the ethyl groups, with the strongest current pattern, obtained when the substrate probe is below an ethyl group, producing asymmetric lobes.

Therefore, with the assumption that the ethyl groups of the molecule point away from the substrate, the different transmission pattern results obtained experimentally, showing four asymmetric lobes, can clearly still be reproduced within our model.

IV. CONCLUSIONS

We have explored theoretically a model of scanning tunneling microscopy in which a molecule is contacted with two *local* probes, one representing the STM tip and the other the substrate. This is the simplest model of STM of large molecules separated from conducting substrates by thin insulating films where the dominant conducting pathway through the insulating film is localized to a region smaller than the molecule.

We have applied this model to Zn(II)-etioporphyrin I molecules on a thin insulating alumina layer. In recent experiments on this system, very different topographic maps were obtained for molecules at different locations on the substrate. We have shown that differences in the details of the effective molecule-substrate coupling due to the non-uniform transmission of electrons through the alumina can account for the differences in topographic maps of these molecules. Our model results suggest that the out-of-plane ethyl groups of the molecule may be the location of dominant molecule-probe coupling.

Our theory also suggests that further experiments in which the molecules are on a thin alumina film over an NiAl(111) substrate (complementing the work in Ref. 16 with the NiAl(110) substrate) would be of interest: Unlike thin alumina films on NiAl(110) substrates,³⁰ thin alumina films on NiAl(111) substrates have *periodic* arrays of spots at which electron transmission through the alumina is enhanced.²⁹ Thus for Zn(II)-etioporphyrin I molecules on alumina/NiAl(111) it may be possible to observe simultaneously both the periodic array of spots where transmission through the alumina is enhanced and the STM images of molecules on the surface and to study experimentally the interplay between the two in a controlled way.

Studying the scanning tunneling microscopy of molecules using a framework of two local probes opens a new avenue for future theoretical and experimental research, and we hope that it will help to achieve a greater understanding of molecular electronic systems.

ACKNOWLEDGMENTS

This research was supported by NSERC and the Canadian Institute for Advanced Research.

REFERENCES

- ¹ H. Ohtani, R. J. Wilson, S. Chiang and C. M. Mate, *Phys. Rev. Lett.* **60**, 2398 (1988).
- ² P. H. Lippel, R. J. Wilson, M. D. Miller, C. Wöll and S. Chiang, *Phys. Rev. Lett* **62**, 171 (1989).
- ³ J. A. Stroscio and D. M. Eigler, *Science* **254**, 1319 (1991).
- ⁴ C. Joachim, J. K. Gimzewski, R. R. Schlittler and C. Chavy, *Phys. Rev. Lett.* **74**, 2102 (1995).
- ⁵ S. Datta, W. Tian, S. Hong, R. Reifenberger, J. I. Henderson and C. P. Kubiak, *Phys. Rev. Lett.* **79**, 2530 (1997).
- ⁶ J. K. Gimzewski and C. Joachim, *Science* **283** 1683 (1999).
- ⁷ W. Ho, *J. Chem. Phys.* **117**, 11033 (2002).
- ⁸ A. J. Fisher and P. E. Blöchl, *Phys. Rev. Lett.* **70**, 3263 (1993).
- ⁹ F. Biscarini, C. Bustamante and V. M. Kenkre, *Phys. Rev. B* **51**, 11089 (1995).
- ¹⁰ P. Sautet and M. L. Bocquet, *Phys. Rev. B* **53**, 4910 (1996).
- ¹¹ P. Sautet, *Chem. Rev.* **97** 1097 (1997).
- ¹² X. Lu and K. W. Hipps, *J. Phys. Chem. B* **101**, 5391 (1997).
- ¹³ T. A. Jung, R. R. Schlittler and J. K. Gimzewski, *Nature* **386**, 696 (1997).
- ¹⁴ M. Schunack, F. Rosei, Y. Naitoh, P. Jiang, A. Gourdon, E. Laegsgaard, I. Stensgaard, C. Joachim and F. Besenbacher, *J. Chem. Phys.* **117**, 6259 (2002).
- ¹⁵ K. Walzer and M. Hietschold, *Surf. Sci.* **471**, 1 (2001).
- ¹⁶ X. H. Qiu, G. V. Nazin and W. Ho, *Science* **299**, 542 (2003).
- ¹⁷ X. H. Qiu, G. V. Nazin and W. Ho, *Phys. Rev. Lett* **92**, 206102 (2004).
- ¹⁸ Z. C. Dong, X. L. Guo, A. S. Trifonov, P. S. Dorozhkin, K. Miki, K. Kimura, S. Yokoyama and S. Mashiko, *Phys. Rev. Lett.* **92**, 86801 (2004).
- ¹⁹ J. Repp, G. Meyer, S. M. Stojkovic, A. Gourdon and C. Joachim, *Phys. Rev. Lett* **94**, 26803 (2005).
- ²⁰ J. Bardeen, *Phys. Rev. Lett.* **6**, 57 (1961).
- ²¹ J. Tersoff and D. R. Hamann, *Phys. Rev. Lett.* **50**, 1998 (1983); *Phys. Rev. B* **31**, 805 (1985).
- ²² P. Sautet and C. Joachim, *Phys. Rev. B* **38**, 12238 (1988).
- ²³ G. Doyen, E. Koetter, J. P. Vigneron and M. Scheffler, *Appl. Phys. A* **51**, 281 (1990).
- ²⁴ W. Sacks and C. Noguera, *Phys. Rev. B* **43**, 11612 (1991).
- ²⁵ M. Tsukada, K. Kobayashi, N. Isshiki and H. Kageshima, *Surf. Sci. Rep.* **13**, 265 (1991).
- ²⁶ J. P. Vigneron, I. Derycke, P. Lambin, T. Laloyaux, A. A. Lucas, L. Libioulle and A. Ronda, *Ultramicroscopy*, **42**, 250 (1992).
- ²⁷ V. M. Kenkre, F. Biscarini and C. Bustamante, *Phys. Rev. B* **51**, 11074 (1995).
- ²⁸ J. Buker and G. Kirczenow, *Phys. Rev. B* **66** 245306 (2002).
- ²⁹ T. Maroutian, S. Degen, C. Becker, K. Wandelt, and R. Berndt, *Phys. Rev. B* **68**, 155414 (2003).
- ³⁰ G. Kresse, M. Schmid, E. Napetschnig, M. Shishkin, L. Köhler and P. Varga, *Science* **308**, 1440 (2005).
- ³¹ In this work we are considering thin, mainly planar molecules oriented parallel to the substrate. In this geometry most of the potential drop occurs in the insulating layer between the metal substrate and the molecule, and between the molecule and the STM

tip. Thus to a first approximation the potential drop within the molecule itself can be neglected.

³² The implementation used was that of G. A. Landrum and W. V. Glassy, YAeHMOP project, <http://yaehmop.sourceforge.net>

³³ E. Emberly and G. Kirczenow, Phys. Rev. Lett. **81**, 5205 (1998); J. Phys.: Condens. Matter **11**, 6911 (1999).

³⁴ The B3PW91 functional and Lanl2DZ basis set were used for this calculation. M. J. Frisch, G. W. Trucks, H. B. Schlegel *et al.*, GAUSSIAN 98, Gaussian, Inc, Pittsburgh, PA, 1998.

³⁵ E. G. Emberly and G. Kirczenow, Phys. Rev. B **58**, 10911 (1998).

³⁶ M. Di Ventura, S. T. Pantelides and N. D. Lang, Phys. Rev. Lett. **84**, 979 (2000).

³⁷ P. S. Damle, A. W. Ghosh and S. Datta, Phys. Rev. B **64**, 201403(R) (2001).

³⁸ This value is predicted by an extended Hückel cluster calculation for a Cu probe.

³⁹ As is discussed in Section III C, in the relevant experiments,¹⁶ the molecular LUMO (HOMO) state is probed when the tip is biased negatively (positively) relative to the substrate.

⁴⁰ X. H. Qiu, G. V. Nazin and W. Ho, Phys. Rev. Lett. **93**, 196806 (2004).

⁴¹ Here we have assumed for simplicity that processes injecting electrons into different ethyl groups are mutually incoherent.

FIGURES

FIG. 1. Illustrative diagram for an STM/molecule/substrate experiment, showing a possible pathway for electron transmission when the molecule is weakly bound to the substrate due to the presence of a complex insulating layer that transmits electrons non-uniformly. A region of dominant molecule-substrate coupling causes electron transmission to occur primarily through a single pathway.

FIG. 2. Illustration of a two-probe theory of scanning tunneling microscopy. Tip and substrate are both considered to be local probes coupled to the molecule.

FIG. 3. A schematic diagram of the model STM/molecule/substrate system. The tip and substrate probes are semi-infinite. Nearest neighbour atoms to the molecule (with atomic orbitals labelled $|a\rangle$ and $|b\rangle$) are considered to be part of the *extended molecule*, which is represented by the dashed rectangle.

FIG. 4. (color online). The Zn(II)-etioporphyrin I molecule. Carbon atoms are red, nitrogen atoms are green, the zinc atom is yellow, and hydrogen is white. The four blue circles (labelled A, B, C, and D) denote four possible positions for the substrate probe below the molecule (into the page), that are considered in this article. In each case, the closest atom in the substrate probe (atomic orbital $|b\rangle$ in Fig. 3) is 2.5\AA below the nearest atom of the molecule.

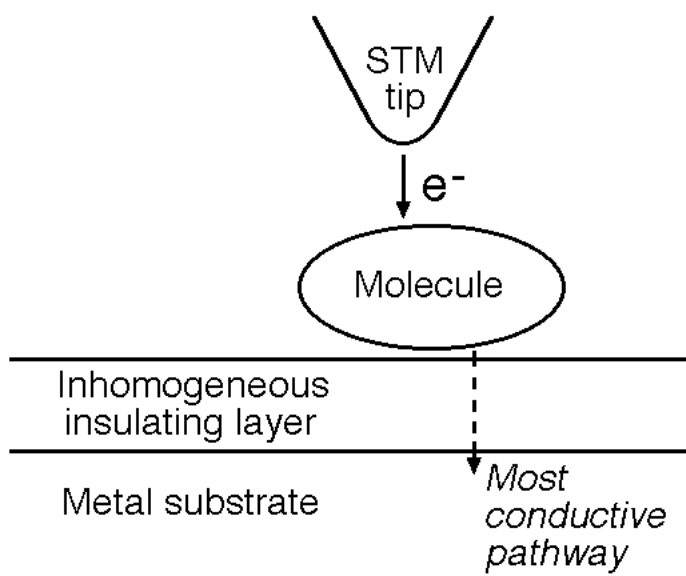
FIG. 5. (color online). Transmission at LUMO energies. a,b,c,d) $16\text{\AA}\times 16\text{\AA}$ constant-height transmission patterns, for 4 different substrate probe positions. Darker regions represent tip probe positions that give higher current flow through the molecule. The blue circles represent the position of the substrate probe below the molecule in each case, the closest atom of the probe being 2.5\AA below the nearest atom of the molecule. These positions correspond to the blue circles in Fig. 4: a)circle A, b)circle B, c)circle C, d)circle D. The red dots represent tip probe positions for the corresponding $T(E)$ curves shown in e,f,g,h respectively. e) Transmission vs. energy for tip and substrate probes directly above and below an outer ethyl group. f) $T(E)$ for the tip probe above the same ethyl group but the substrate probe below an inner corner carbon atom. g) $T(E)$ for tip and substrate probes above and below a nitrogen atom. h) $T(E)$ for tip and substrate probes above and below the central zinc atom. In all cases, the tip probe is 2.5\AA above the plane of the molecule.

FIG. 6. The same $16\text{\AA}\times 16\text{\AA}$ transmission pattern shown in Fig. 5d, with transmission plotted on a Log scale. Additional delocalized features can be seen.

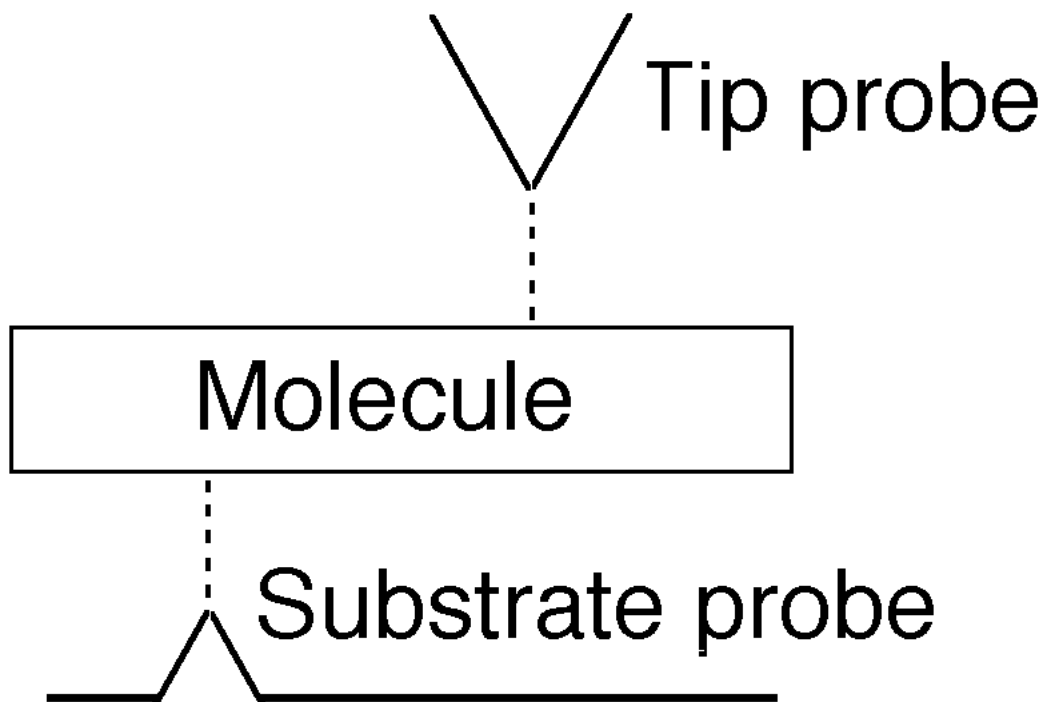
FIG. 7. (color online) Transmission at HOMO energies. a,b,c,d) $16\text{\AA} \times 16\text{\AA}$ constant-height transmission patterns, for 4 different substrate probe positions. As in Fig. 5, the blue circles represent the position of the substrate probe below the molecule. Again, they correspond to the blue circles in Fig. 4: a) circle A, b) circle B, c) circle C, d) circle D. The red dots represent tip probe positions for the corresponding $T(E)$ curves shown in e,f,g,h respectively. An additional black dot just below the red dot in (a) represents a different tip probe position, yielding a second $T(E)$ curve in e). e) $T(E)$ for the substrate probe directly below an outer ethyl group, and the tip probe on a low transmission node [red curve, red dot in (a)], or close to this node [black curve, black dot in (a)]. The narrow transmission peak near -11.9 eV exists for both curves (the black curve is under the red curve). Note that the energy scale is different than for f,g,h. f) $T(E)$ for the tip and substrate probes above and below an inner corner carbon atom. g) $T(E)$ for tip and substrate probes above and below a nitrogen atom. h) $T(E)$ for tip and substrate probes above and below the central zinc atom. In all cases, each probe is 2.5\AA away from the nearest atom in the molecule.

FIG. 8. The $16\text{\AA} \times 16\text{\AA}$ transmission pattern shown in Fig. 5a, in convolution with a gaussian weighting function of width 6\AA . This is done in order to more realistically simulate what one might expect to see in a real STM experiment. Two distinct asymmetric lobes are visible, and the calculated pattern is similar to the most common STM image observed experimentally by Qiu *etal.*¹⁶ which is shown in Fig. 2B of their paper.

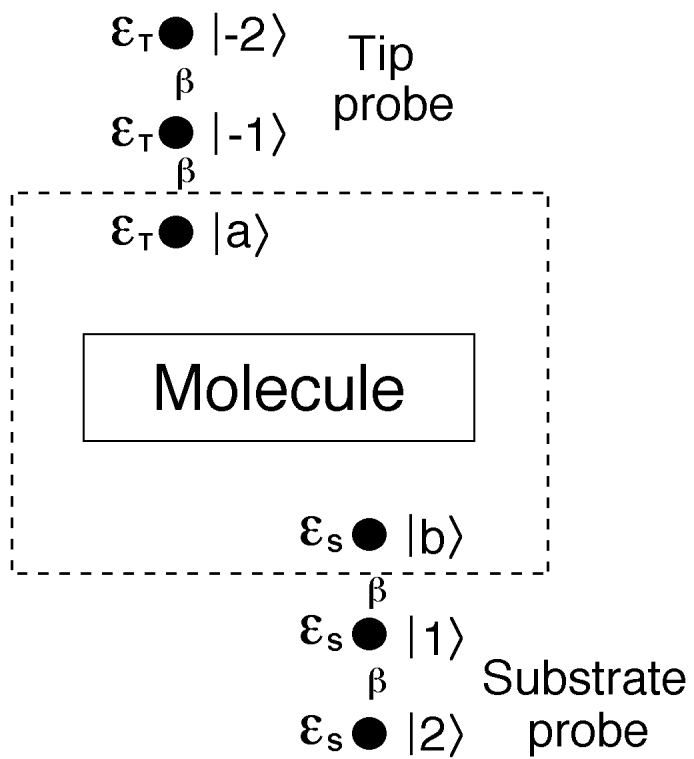
FIG. 9. Transmission at LUMO energies, assuming ethyl groups point *away* from the substrate probe. a,b,c,d) $16\text{\AA} \times 16\text{\AA}$ transmission patterns for the 4 different substrate probe positions shown in Fig. 4: a) circle A, b) circle B, c) circle C, d) circle D. The substrate probe is in all cases 2.5\AA below the plane of the molecule, and the tip probe is 4.0\AA above the plane of the molecule.



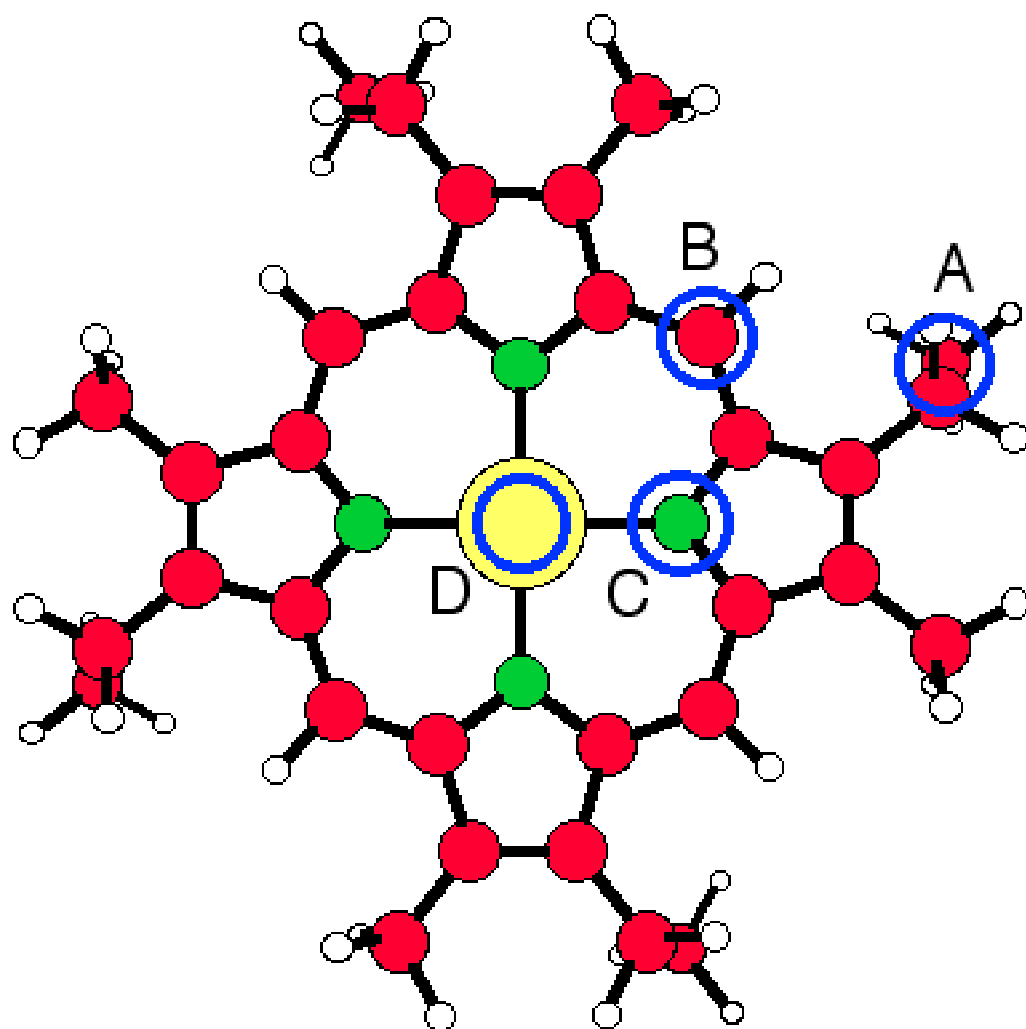
Buker and Kirczenow, Fig. 1



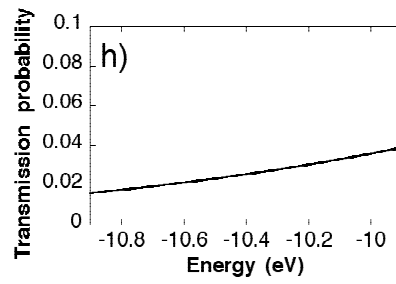
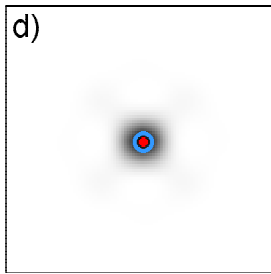
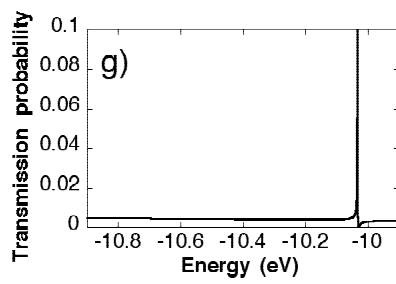
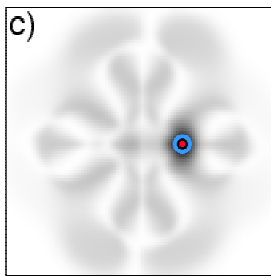
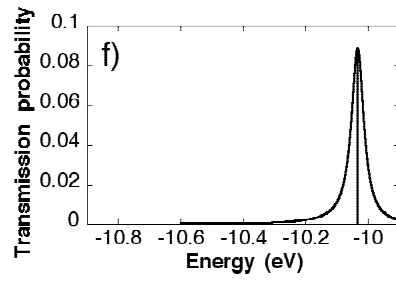
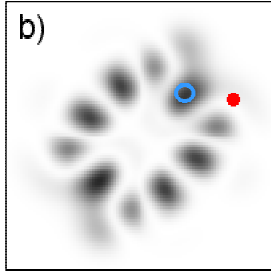
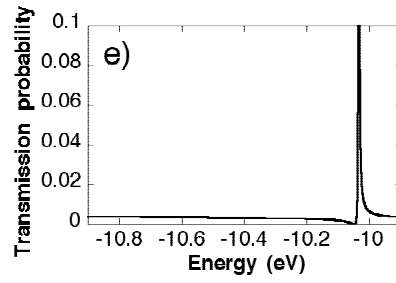
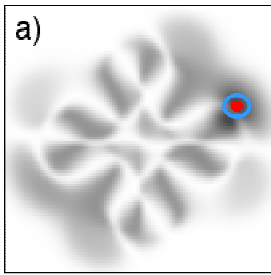
Buker and Kirczenow, Fig. 2



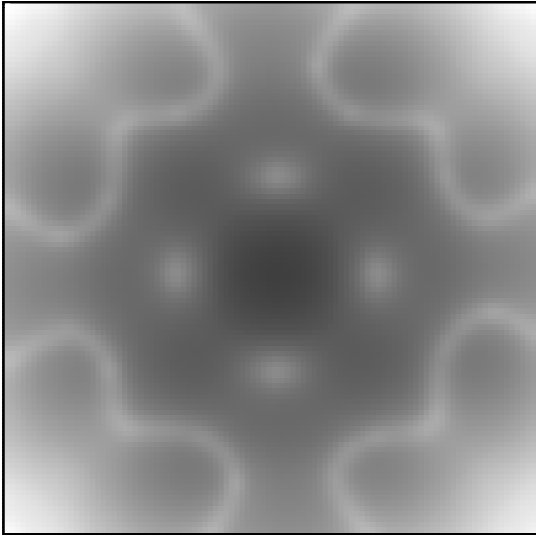
Buker and Kirczenow, Fig. 3



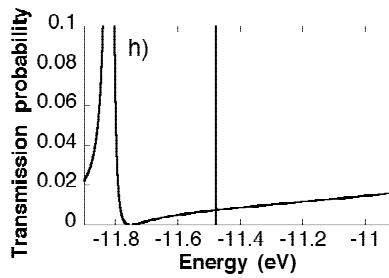
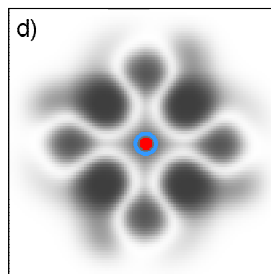
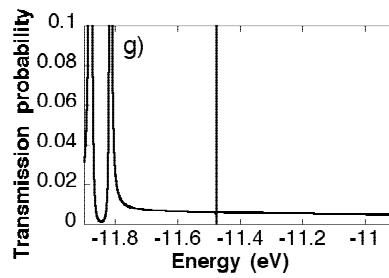
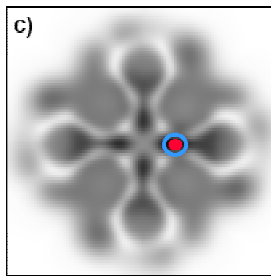
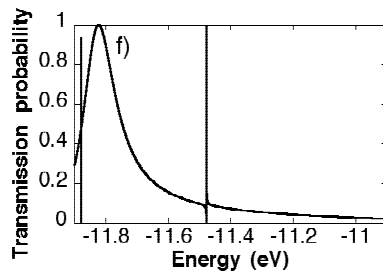
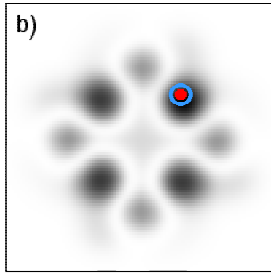
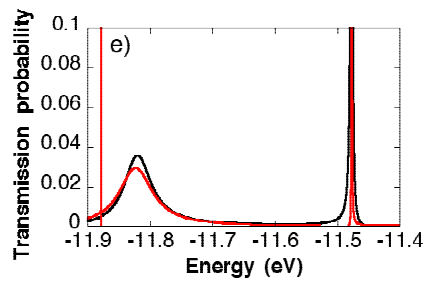
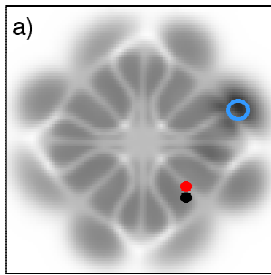
Buker and Kirczenow, Fig. 4



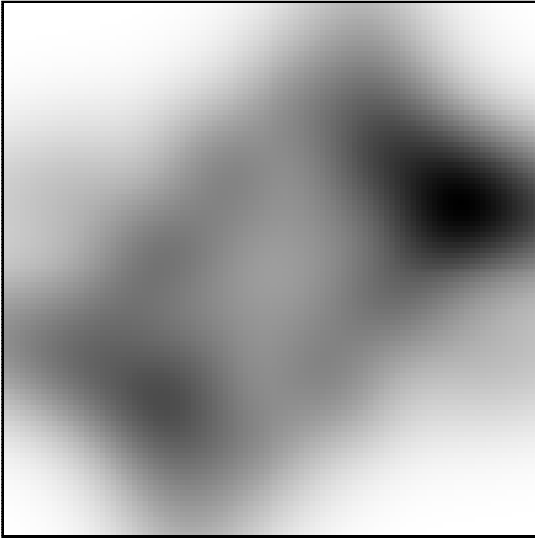
Buker and Kirczenow, Fig. 5



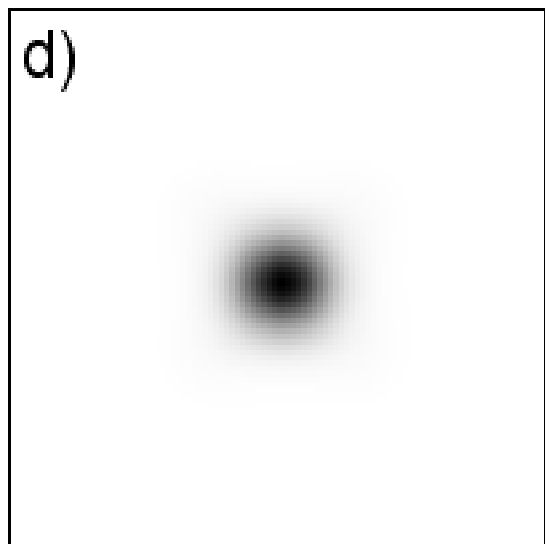
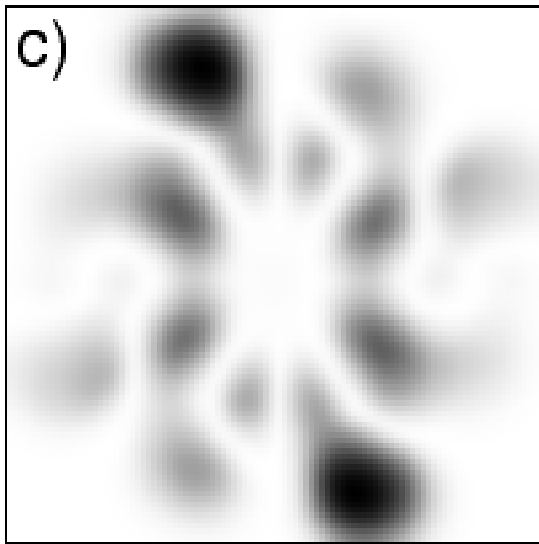
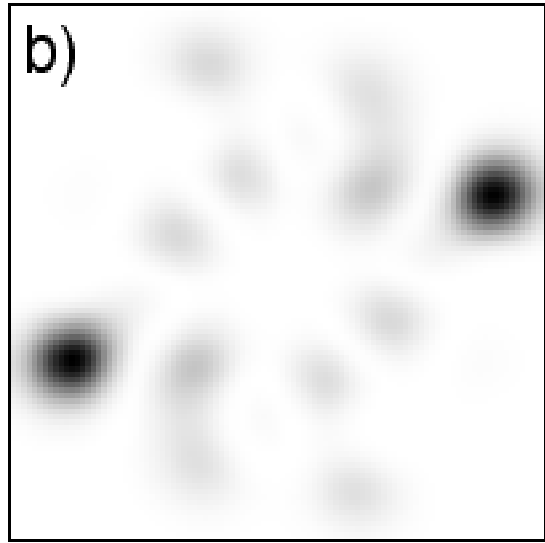
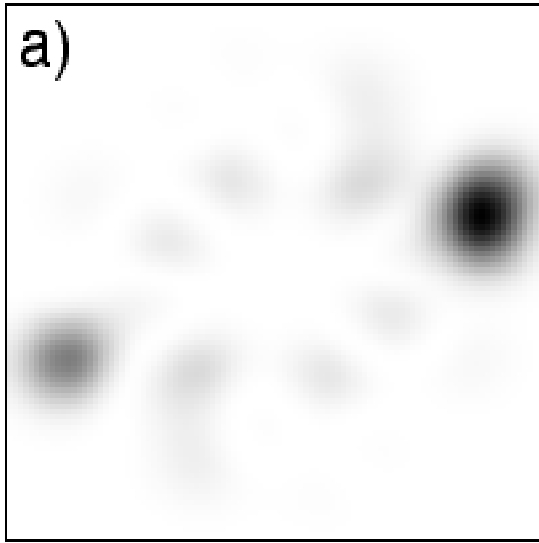
Buker and Kirczenow, Fig. 6



Buker and Kirczenow, Fig. 7



Buker and Kirczenow, Fig. 8



Buker and Kirczenow, Fig. 9